A Study on the Anode Effect in KF-2HF System. III. Influence of Bath Temperature and Surface Tension and Addition of Fluoride Particles on the Occurrence of the Anode Effect

Hiroki IMOTO, Kazuo UENO, and Nobuatsu WATANABE*

Department of Industrial Chemistry, Faculty of Engineering, Kyoto University, Yoshida, Sakyo-ku, Kyoto 606

(Received March 24, 1978)

The decomposition reaction of the graphite fluoride film formed on the edge plane of pyrolytic graphite, carbon, and graphite electrodes was faster in a KF·HF bath (250 °C) than in a KF·2HF bath (100 °C) due to the higher temperature of KF·HF bath. The critical current densities (CCD's)[1] were about 0.1 A/cm² for the layer and edge planes of pyrolytic graphite, carbon, and graphite electrodes in the KF·HF bath, and the CCD for each electrode was larger in the KF·HF bath than in the KF·2HF bath. The anode effect took place easily on the glassy carbon electrode in the KF·2HF bath. However, the anode effect did not take place in liquid hydrogen fluoride due to its very low surface tension, although the graphite fluoride film was formed on the electrode surface. The zeta-potential of aluminum fluoride particles in liquid hydrogen fluoride containing 0—20 mol of potassium fluoride/l and that of magnesium fluoride particles in liquid hydrogen fluoride were almost zero at 0 °C. From the results it is not proper that the effect of the addition of dispersed particles upon the anode effect is explained by the view of electrostatic force of the particles proposed so far.[2]

The anodic behavior of four kinds of electrodes (graphite, carbon, pyrolytic graphite, and glassy carbon) have been investigated in KF·2HF bath.[2-4] It has been suggested that the occurrence of the anode effect is influenced by the wettability of the anode surface with the bath and the kinetic balance of the rates of the formation and decomposition reaction of the graphite fluoride, $(CF)_n$,[5] film on the anode. The wettability and the kinetic balance vary with the surface tension and the operating temperature of the bath, respectively. Table 1 shows the surface tensions of the KF–HF system. The surface tension of liquid hydrogen fluoride (LHF, 0 °C) is much lower than that of KF·2HF melt (100 °C). The surface tension of KF·HF melt (250 °C) is almost the same as that of KF·2HF melt. Therefore, in the present study, LHF and KF·HF melt were used as baths for investigating the influence of the surface tension and the temperature of the baths on the occurrence of the anode effect.

TABLE 1. SURFACE TENSION OF KF–HF SYSTEM

	LHF[a]	KF·2HF[b]	KF·HF[c]
Temperature (°C)	0	100	245
Surface tension (dyn/cm)	10	95	118
Temperature coefficient of surface tension (dyn/cm °C)	−0.08	−0.1	

a) H. H. Hyman, and J. J. Katz, "Non-Aqueous Solvent Systems," ed by T. C. Waddington, Academic Press, London and New York (1965), p. 53. b) N. Watanabe, M. Ishii, and S. Yoshizawa, *Denki Kagaku*, **29**, 492 (1961). c) A. J. Rudge, "Industrial Electrochemical Processes," ed by A. T. Kuhn, Elsevier Publishing Company, Amsterdam-London-New York (1971), p. 12.

The addition of lithium fluoride, nickel fluoride, aluminum fluoride, calcium fluoride,[6] magnesium fluoride[7] particles to the KF·2HF bath is effective for preventing the anode effect. This effect has been explained on the basis of the zeta-potential of the fluoride particles.[2] In order to confirm the explanation proposed, the zeta-potentials of aluminum fluoride (AlF_3) and magnesium fluoride (MgF_2) particles dispersed in KF–HF system were measured at 0 °C.

Experimental

The cell was kept at 100 and 250 °C for KF·2HF and KF·HF baths, respectively. A platinum rod was used as a reference electrode in both baths. Further detailed descriptions of the apparatus and the procedure for the measurement in the KF·2HF bath have been given in previous papers.[4,8] The measurement in the KF·HF bath was the same as that in the KF·2HF bath. The electrolytic cell for LHF was identical to that reported before[9] and cooled at 0 °C in ice bath. The Cu/CuF_2 electrode was used as a reference electrode, and a nickel plate as a counter electrode. Small amounts of potassium fluoride were added to LHF as a supporting electrolyte. LHF in the cell was dehydrated by pre-electrolysis with nickel electrodes for 2 days. The glassy carbon electrode was connected with a nickel lead by winding fine copper wires. The nickel lead and all parts of the glassy carbon except for the working electrode surface were protected with perflon paint[10] and Teflon (poly(tetrafluoro-

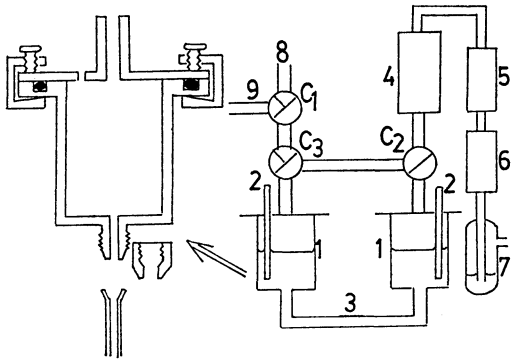

Fig. 1. Apparatus for the measurement of zeta-potential (microelectrophoresis cell).
1: Electrolytic cell, 2: electrode (nickel), 3: transparent pipe (Kel-F), 4: reflux condenser (methanol at −20 °C), 5: HF absorber (NaF pellets), 6: silica gel, 7: atmospheric seal, 8: HF inlet, 9: N_2 inlet, C_1, C_2, and C_3: Teflon stopcocks.

ethylene)) tape. Before ESCA measurement, the electrode of pyrolytic graphite was washed with LHF in order to remove the KF·HF remaining on the electrode. The ESCA spectrum of C 1s electron for the electrode has two peaks at 284 and 288.5 eV.[8] The former peak corresponds to the binding energy of the C 1s electron for the carbon atom which has only the C–C bond, and the latter peak corresponds to the one for the carbon atom with C–F bond. The height of the peaks at 284 and 288.5 eV were represented by h_0 and h_1, respectively and the value of $h_1/(h_0+h_1)$ was adopted as the relative amount of $(CF)_n$ on the electrode surface. The zeta-potential of particles dispersed in the KF–HF system was measured using a microelectrophoresis apparatus as shown in Fig. 1. The cell was specially designed for the corrosive hydrogen flouride, that is, the microscopic observation tube (3) was made of transparaent poly(trifluorochloroethylene) and the other parts were made of Teflon. The parts (1), (2), and (3) in Fig. 1 were kept at 0 °C in a cold air bath. The potential gradient between the nickel electrodes (2) was varied from 0 to 2.7 V/cm.

Results and Discussion

Effect of the Temperature of Bath. Figure 2 shows the *I-V* curves obtained by the linear potential sweep method for the layer plane (G_L) and edge plane (G_E) of the pyrolytic graphite electrodes in the KF·HF bath at 250 °C. The potential of the electrode G_L or G_E was swept from 0 to 7.0 V *vs.* Pt (forward sweep) and subsequently from 7 to 3.5 V (backward sweep). Two peaks were observed on both curves (a) and (b) on the forward sweep. This may be explained in terms of formation of two kinds of $(CF)_n$ films on the anode surface,[3] that is, the $(CF)_n$ film which has extremely low surface energy is formed at the second peak, and the current decreases rapidly with increasing potential. But the current restored on the backward sweep only on the electrode G_E, indicating that decomposition took place easily on the electrode. The peak current densities on the forward (second peak) and the backward sweeps were represented by P_f and P_b, respectively. The value of P_b/P_f for the electrode G_E was about twice as large in the KF·HF bath as in the KF·2HF bath, because the former cell temperature was about 150 °C higher than the latter one and therefore the $(CF)_n$ film easily decomposed in the KF·HF bath.[11] On the other hand, the current was hardly restored on the backward sweep on the electrode G_L, which means that the $(CF)_n$ film on the electrode G_L was hardly decomposed.

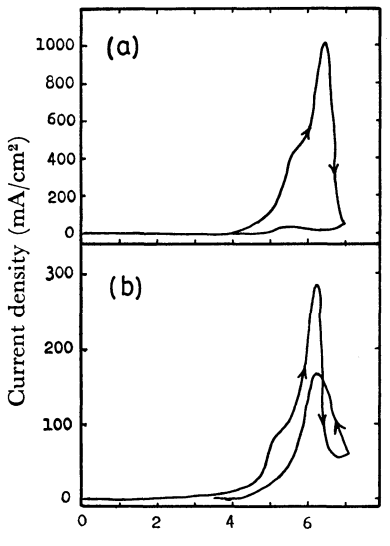

Fig. 2. *I-V* curves (potential sweep) in KF·HF bath at 250 °C.
Anode: (a) electrode G_L, (b) electrode G_E, potential sweep rate: 50 mV/s.

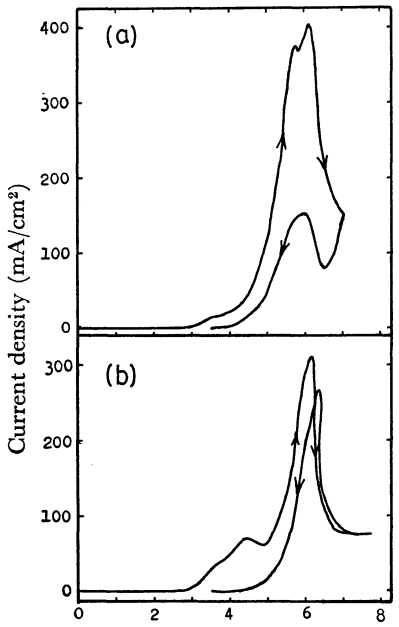

Fig. 3. *I-V* curves (potential sweep) in KF·HF bath at 250 °C.
Anode: (a) graphite, (b) carbon, potential sweep rate: 50 mV/s.

Figure 3 shows the *I-V* curves for the commercial carbon and graphite electrode. The values of P_b/P_f for the graphite and carbon electrodes were two and three times larger in the KF·HF bath than in KF·2HF bath, respectively. Consequently, the rate of decomposition of the $(CF)_n$ film on the anode surface is faster in KF·HF bath than in the KF·2HF bath when the electrode G_E and the carbon and graphite electrodes are used as anodes.

Figure 4 shows the potential sweep rate dependence of the P_f value for the four kinds of electrodes mentioned above. The dependence of the P_f values for these electrodes on the potential sweep rate showed the same tendency in both the KF·2HF and the KF·HF baths. Only the peak current density for the electrode G_L increased with the potential sweep rate much more than those for the other electrodes. From previous discussion,[4] this indicates that the covering rate of the electrode surface with the $(CF)_n$ was slower on the electrode G_L than on the other electrodes. Furthermore, the peak current densities for the four kinds of electrodes were independent of potential sweep rate within the

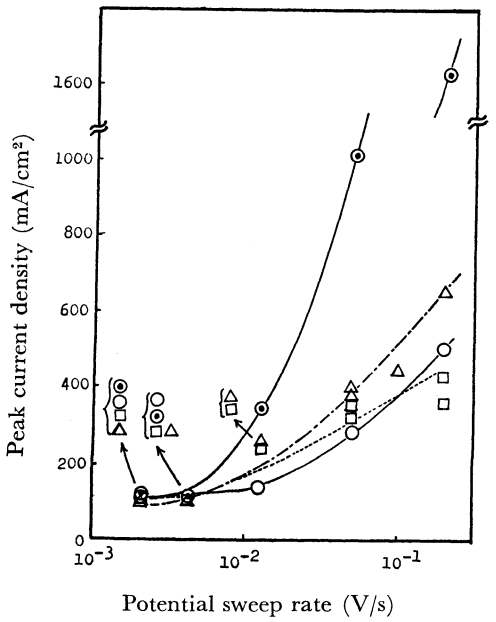

Fig. 4. Dependence of peak current densities on potential sweep rate in KF·HF bath (250 °C).
⊙ Electrode G_L, ○ electrode G_E, △ graphite, □ carbon.

region of low sweep rate. As the steady state condition was established within the region, the critical current densities (CCD's)[1] were found to be about 0.1 A/cm² for all electrodes from the peak current densities. The CCD's for the carbon, graphite, G_L, and G_E electrodes in the KF·2HF bath were 80, 25, 20, and 55 mA/cm², respectively. From the results, the KF·HF bath has advantages for operating the fluorine cell at higher current density compared with the KF·2HF bath.

When the electrode G_L or G_E was potentiostatically polarized in the KF·HF bath, the current reached a stationary value within 10 min. The ESCA spectra of C 1s electron for these electrodes were obtained after the polarization. The potential dependence of the values of $h_1/(h_0+h_1)$ is shown in Fig. 5. The potential

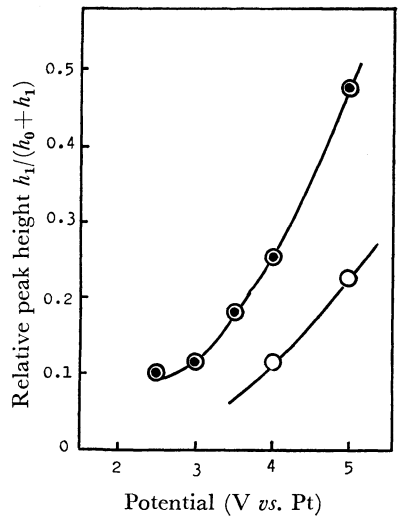

Fig. 5. Potential dependence of ESCA spectra of C 1s electron for pyrolytic graphite anode surface.
⊙ Electrode G_L, ○ electrode G_E.

dependence of the amount of the $(CF)_n$ film formed on the electrode G_L in the KF·HF bath was similar to that in the KF·2HF bath. However the $(CF)_n$ film was hardly observed on the electrode G_L polarized at lower potential than 3.5 V, although the $(CF)_n$ film was formed on the electrode polarized at 2 V in the KF·2HF bath. These facts suggest that the $(CF)_n$ formed on the electrode G_E at lower potential was easily decomposed due to the higher temperature of the KF·HF bath and the film on the electrode G_L was thermally more stable than that on the electrode G_E. These results may support the interpretation of the *I-V* curves described above.

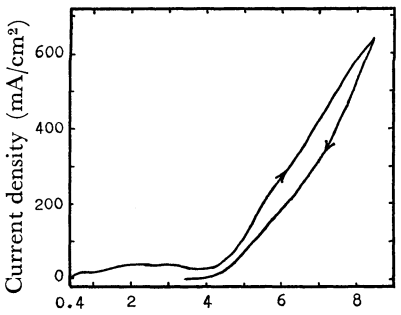

Fig. 6. *I-V* curve (potential sweep) in liquid hydrogen fluoride at 0 °C.
Electrode: glassy carbon, potential sweep rate: 12.5 mV/s.

Effect of Surface Tension of Bath. Only the polarization curve of the glassy carbon electrode could be obtained even in the LHF bath.[12] Figure 6 shows *I-V* curve for the glassy carbon electrode obtained by the linear potential sweep method at the potential between 0.4—8.4 V (the potential is converted into the potential *vs.* hydrogen electrode only in this section). The *I-V* curve obtained in the LHF bath was significantly different from that obtained in the KF·2HF bath, since the current increased with increasing potential without the anode effect becoming apparent. On the other hand, the current decreased rapidly at about 5.5 V with increasing potential due to the anode effect in the KF·2HF bath. The ESCA spectrum of C 1s electron for the surface of the glassy carbon electrode polarized at 4.9 V for 10 min in the LHF bath indicated the existence of the $(CF)_n$ film on the electrode surface. When the $(CF)_n$ film is formed on the glassy carbon electrode by the anodic polarization in the KF·2HF bath, the anode effect takes place, because the elctrode does not come into direct contact with the bath due to the high surface tension of the bath. However, the anode effect does not take place in the LHF bath in spite of the formation of the $(CF)_n$ film on the electrode, because the electrode surface comes into contact with the bath due to the very low surface tension of the LHF bath. The results verify the mechanism of the occurrence of the anode effect proposed,[2,13,14] and agree with the fact that when the carbon anode is used, the CCD's are 50—60 and 60—80 mA/cm² in KF·2HF (100 dyn/cm, 90 °C) and KF·3HF (75 dyn/cm, 80 °C) baths, respectively.[2]

Effect of Addition of Fluoride Particles. The following explanation was proposed[15,16] to account for the suppressive effect of fluoride particles on the anode effect. If the fluorine gas bubbles generated on the anode have negative charges, it is difficult for the bubbles to be separated from the anode because of the electrostatic attractive forces. If the colloidal fluoride particles have positive charges, they would be absorbed on the fluorine bubbles to neutralize the negative charges of the bubbles. Consequently the electrostatic force between the fluorine gas bubbles and the anode becomes remarkably weak and the fluorine gas bubbles can be readily separated from the anode surface. The zeta-potential of AlF_3 and MgF_2 particles dispersed in the KF–HF system were measured. The zeta-potentials of AlF_3 in LHF containing 0—20 mol of potassium fluoride/l and of MgF_2 in LHF were almost zero at 0 °C. Therefore, the zeta-potentials of AlF_3 and MgF_2 particles are thought to be almost zero in the KF·2HF bath of which the ionic strength is very high. From the results, it was found that the suppressive effect of the dispersed fluoride particles upon the anode effect cannot be accounted for in terms of the electrostatic interaction proposed so far.

Conclusion

1) The rate of decomposition of the graphite fluoride film formed on the edge plane of pyrolytic graphite, carbon, and graphite anodes was faster in the KF·HF bath than in the KF·2HF bath, and each critical current density for the pyrolytic graphite, carbon, and graphite electrodes was higher in the KF·HF bath than in the KF·2HF bath.

2) The anode effect did not take place in liquid hydrogen fluoride due to the very low surface tension of liquid hydrogen fluoride, which verifies the mechanism of the anode effect in KF·2HF bath proposed so far.

3) It was found that the suppressive effect of the dispersed fluoride particles upon the anode effect cannot be explained from the view of electrostatic force proposed so far.

References

1) An value of current density for the tendency to the occurrence of the anode effect. Anode effect takes place inevitably above the current density.

2) N. Watanabe, M. Ishii, and S. Yoshizawa, *Denki Kagaku*, **29**, 497 (1961).

3) M. Nishimura, A. Tasaka, K. Nakanishi, and N. Watanabe, *Denki Kagaku*, **38**, 294 (1970).

4) H. Imoto and N. Watanabe, *Bull. Chem. Soc. Jpn.*, **49**, 1736 (1976).

5) $(CF)_n$ has very low surface energy. See N. Watanabe, H. Takenaka, and S. Kimura, *Nippon Kagaku Kaishi*, **1975**, 1655.

6) N. Watanabe, M. Ishii, and S. Yoshizawa, *Denki Kagaku*, **29**, 492 (1961).

7) A. J. Rudge, "Industrial Electrochemical Processes," ed by A. T. Kuhn, Elsvier publishing Co., Amsterdam-London-New York (1971), p. 25.

8) H. Imoto and N. Watanabe, *Bull. Chem. Soc. Jpn.*, **48**, 1633 (1975).

9) M. Haruta and N. Watanabe, *J. Fluorine Chem.*, **7**, 159 (1976).

10) The fluorine-contained rubber dissolved in 2-butanone.

11) H. Imoto and N. Watanabe, *Denki Kagaku*, being submitted.

12) A. G. Doughty, M. Fleishmann, and D. Pletcher, *Electroanal. Chem. Interf. Electrochem.*, **51**, 456 (1974).

13) N. Watanabe, Y. Fujii, and S. Yoshizawa, *Denki Kagaku*, **31**, 611 (1963).

14) N. Watanabe, F. Kato, and K. Omura, *Denki Kagaku*, **37**, 274 (1969).

15) N. Watanabe, M. Inoue, and S. Yoshizawa, *Denki Kagaku*, **31**, 698 (1963).

16) N. Watanabe and N. Ooba, *Denki Kagaku*, **35**, 178 (1967).